NATIONAL ENERGY TECHNOLOGY LABORATORY
OIL & GAS

DOE Award No.: DE-FE-0028967

Quarterly Research Performance Progress Report (Period Ending 6/30/2019)

A multi-scale experimental investigation of flow properties in coarse-grained hydrate reservoirs during production

Project Period (10/1/2016-9/30/2019)

Submitted by:
Peter B. Flemings

DocuSigned by:
Peter B. Flemings
36634B8D9FFC496...
Signature

The University of Texas at Austin
DUNS #: 170230239
101 East 27th Street, Suite 4.300
Austin, TX 78712-1500
Email: pflemings@jsg.utexas.edu
Phone number: (512) 475-8738

Prepared for:
United States Department of Energy
National Energy Technology Laboratory

July 30, 2019

U.S. DEPARTMENT OF ENERGY | NATIONAL ENERGY TECHNOLOGY LABORATORY

Office of Fossil Energy

DISCLAIMER

1. ACCOMPLISHMENTS:

What was done? What was learned?

This report outlines the progress of the third quarter of the third fiscal year in the second budget period. Highlights from the period include:

- We completed revisions on our paper on depressurization of methane hydrate-bearing sand packs, and it was accepted in final form on June 7 (see 2. Products).
- We continue to develop a systematic approach to explore 3-phase permeability (hydrate, vapor, and water). Our initial results suggest that hydrate is behaving as a non-wetting phase (like vapor) and that we can use a simple Brooks-Corey type fit to describe relative permeability.

A. What are the major goals of the project?

The goals of this project are to provide a systematic understanding of permeability, relative permeability and dissipation behavior in coarse-grained methane hydrate - sediment reservoirs. The results will inform reservoir simulation efforts, which will be critical to determining the viability of the coarse-grained hydrate reservoir as an energy resource. We will perform our investigation at the macro- (core) and micro- (pore) scale.

At the macro- (core) scale, we will: 1) measure the relative permeability of the hydrate reservoir to gas and water flow in the presence of hydrate at various pore saturations; and 2) depressurize the hydrate reservoir at a range of initial saturations to observe mass transport and at what time scale local equilibrium describes disassociation behavior. Simultaneously, at the micro (pore) scale, we will 1) use micro-CT to observe the habit of the hydrate, gas, and water phases within the pore space at a range of initial saturations and then image the evolution of these habits during dissociation, and 2) use optical micro-Raman Spectroscopy to images phases and molecules/salinity present both at initial saturations and at stages of dissociation. We will use our micro-scale observations to inform our macro-scale observations of relative permeability and dissipation behavior.

In Phase 1, we first demonstrated our ability to systematically manufacture sand-pack hydrate samples at a range of hydrate saturations. We then measured the permeability of the hydrate-saturated sand pack to flow a single brine phase and depressurized the hydrate-saturated sand packs and observed the kinetic (time-dependent) behavior. Simultaneously we built a micro-CT pressure container and a micro-Raman Spectroscopy chamber and imaged the pore-scale habit, phases, and pore fluid chemistry of sand-pack hydrate samples. We then made observations on our hydrate-saturated sand-packs.

In Phase 2, we will measure relative permeability to water and gas in the presence of hydrate in sand-packs using co-injection of water and gas. We will also extend our measurements from sand-pack models of hydrate to observations of actual Gulf of Mexico material. We will also measure relative permeability in intact samples to be recovered from the upcoming Gulf of Mexico 2017 hydrate coring expedition. We will also perform dissipation experiments on intact Gulf of Mexico

pressure cores. At the micro-scale we will perform micro-Raman and micro-Ct imaging on hydrate samples composed from Gulf of Mexico sediment.

The Project Milestones are listed in the table below.

Milestone Description	Planned Completion	Actual Completion	Verification Method	Comments
Milestone 1.A: Project Kick-off Meeting	11/22/2016 (Y1Q1)	11/22/16	Presentation	Complete
Milestone 1.B: Achieve hydrate formation in sand-pack	6/27/2017 (Y1Q3)	8/11/17	Documentation of milestone achievement within required project reporting / deliverables (Deliverable 2.1)	Complete, *Documentation in the Y1Q3 quarterly and Phase 1 report*
Milestone 1.C: Controlled and measured hydrate saturation using different methods	3/27/2018 (Y2Q2)	3/27/18	Documentation of milestone achievement within required project reporting / deliverables (Deliverable 2.1)	Complete, *Documentation in Y2Q2 quarterly and Phase 1 report*
3 Milestone 1.D: Achieved depressurization and demonstrated mass balance	3/27/2018 (Y2Q2)	12/18/2017	Documentation of milestone achievement within required project reporting / deliverables (Deliverable 3.1)	Complete, *Documentation in the Y2Q1 quarterly and Phase 1 report*
Milestone 1.E: Built and tested micro-consolidation device	6/27/2017 (Y1Q3)	6/27/2017	Documentation of milestone achievement within required project reporting / deliverables (Deliverable 4.1)	Complete, *Documentation in Y1Q3 quarterly and Phase 1 report*
Milestone 1.F: Achieved Hydrate formation and measurements in Micro-CT consolidation device	3/27/2018 (Y2Q2)	2/15/18	Documentation of milestone achievement within required project reporting / deliverables (Deliverable 4.1)	Complete, *Documentation in Y2Q2 quarterly and Phase 1 report*
Milestone 1.G: Built and integrated high-pressure gas mixing chamber	3/27/2018 (Y2Q2)	6/27/17	Documentation of milestone achievement within required project reporting / deliverables (Deliverable 5.1)	Complete, *Documentation in Y1Q3 quarterly and Phase 1 report*
Milestone 1.H: Micro-Raman analysis of synthetic complex methane hydrate	3/28/2018 (Y2Q2)	3/27/18	Documentation of milestone achievement within required project reporting / deliverables (Deliverable 5.1)	Complete, *Documentation in Y2Q2 quarterly and Phase 1 report*
Milestone 2.A - Measurement of relative permeability in sand-pack cores. (See Subtask 6.1)	1/17/2019 (Y3Q2)	expected 9/30/2019	Documentation of milestone achievement within required project reporting / deliverables (Deliverable 6.1)	In progress
Milestone 2.B - Measurement of relative permeability in intact pressure cores. (See Subtask 6.2)	9/30/2019 (Y3Q4)		Documentation of milestone achievement within required project reporting / deliverables (Deliverable 6.1)	
Milestone 2.C -Depressurization of intact hydrate samples and documentation of thermodynamic behavior. (See Subtask 7.1 and 7.2)	9/30/2019 (Y3Q4)		Documentation of milestone achievement within required project reporting / deliverables (Deliverable 7.1)	In progress
Milestone 2.D - Achieved gas production from GOM^2 samples monitored by micro-CT. (See Subtask 8.1 and 8.2)	9/30/2019 (Y3Q4)		Documentation of milestone achievement within required project reporting / deliverables Report (Deliverable 8.1)	In progress

Milestone 2.E - Building a chamber to prepare natural samples for 2D-3D micro-Raman analysis; (See Subtask 9.1 and 9.2)	1/17/2019 (Y3Q2)	3/31/19	Documentation of milestone achievement within required project reporting / deliverables (Deliverable 9.1)	Complete, Documentation in Y3Q3 quarterly and to be included in the Phase 2 report.
Milestone 2.F - 2D micro-Raman analysis of natural methane hydrate samples at depressurization; (See Subtask 9.1 and 9.2)	9/30/2019 (Y3Q4)		Documentation of milestone achievement within required project reporting / deliverables (Deliverable 9.1)	In progress

B. What was accomplished under these goals?

PAST- BUDGET PERIOD 1

Task 1.0 Project Management and Planning

Planned Finish: 09/30/19
Actual Finish: In progress continued in Phase 2, see Task 1 below.

Task 2.0 Macro-Scale: Relative Permeability of Methane Hydrate Sand Packs

Subtask 2.1 Laboratory Creation of Sand-Pack Samples at Varying Hydrate Levels
Planned Finish: 6/ 27/17
Actual Finish: 8/11/17 Complete

Documentation of subtask completion in Y1Q4 Quarterly and the Phase 1 report per the SOPO (Deliverable 2.1).

Subtask 2.2 Steady-State Permeability of Gas and Water of Sand-Pack Hydrate Samples
Planned Finish: 3/27/18
Actual Finish: Complete

Documentation of subtask completion in Y2Q2 Quarterly and the Phase 1 report per the SOPO (Deliverable 2.1).

Task 3.0 Macro-Scale: Depressurization of Methane Hydrate Sand Packs

Subtask 3.1 Depressurization Tests
Planned Finish: 6/27/17
Actual Finish: 3/27/2018 Complete

Documentation of subtask completion in was made in the Phase 1 report per the SOPO (Deliverable 3.1).

Subtask 3.2 Depressurization Tests with CAT scan
Planned Finish: 03/27/18
Actual Finish: 3/27/2018 Complete

Documentation of subtask completion in was made in the Phase 1 report per the SOPO (Deliverable 3.1).

Task 4.0 Micro-Scale: CT Observation of Methane Hydrate Sand Packs

Subtask 4.1 Design and Build a Micro-CT compatible Pressure Vessel
Planned Finish: 6/27/17
Actual Finish: 6/27/2017 Complete

Subtask 4.2 Micro-Scale CT Observations and Analysis
Planned Finish: 03/27/18
Actual Finish: 2/15/2018 Complete

Documentation of Milestone 1.F was included in the Y2 Q2 report and the Phase 1 report per the SOPO (Deliverable 4.1)

Task 5.0 Micro-Scale: Raman Observation of Methane-Gas-Water Systems

Subtask 5.1 Design and Build a Micro-Raman compatible Pressure Vessel
Planned Finish: 6/27/17
Actual Finish: 6/27/17 Complete

Documentation of subtask completion in Y1Q3 Quarterly, Documentation of Milestone 1.G included in the Phase 1 report per the SOPO (Deliverable 5.1)

Subtask 5.2 Micro-scale petrochemistry
Planned Finish: 03/31/18
Actual Finish: 03/27/2018 Complete

Documentation of Milestone 1.H included in the Y2Q2 and Phase 1 report per the SOPO (Deliverable 5.1)

Subtask 5.3 Diffusion kinetics of methane release
Planned Finish: 3/27/18
Actual Finish: 3/27/2018

Documentation of Milestone 1.H included in the Y2Q2 and Phase 1 report per the SOPO (Deliverable 5.1)

Decision Point: Budget Period 2 Continuation

Continuation Application submitted on March 5. Continuation approved March 26, 2018.

CURRENT – BUDGET PERIOD 2

Task 1.0 Project Management and Planning

Planned Finish: 09/30/19
Actual Finish: In progress

This task continues from Phase 1.
The tenth Quarter Report was submitted on May 1, 2019.

Link to actions for next Quarter, Task 1

Task 6.0 Macro-Scale: Relative Permeability of Methane Hydrate Sand Packs and Intact Pressure Core Samples

Subtask 6.1 Steady-State Relative Permeability Measurements of Sand-Pack Hydrate Samples
Planned Finish: 1/17/19
Actual Finish: In Progress, expected 9/30/2019 – we have proposed to spend more time refining the experimental process.

Current understanding of relative permeability in a hydrate-liquid system
The Brooks-Corey model is the most commonly used model for relative permeability as a function of wetting and non-wetting saturation (S_w and S_n) (Brooks and Corey, 1964). The Brooks-Corey model is frequently used in hydrate simulations:

$$k_{rw} = \left(\frac{S_w - S_{rw}}{1 - S_{rw}}\right)^{n_w} \quad (1)$$

$$k_{rn} = \left(\frac{S_n - S_{rn}}{1 - S_{rw}}\right)^{n_n} \quad (2)$$

where S_{rw} is the residual water saturation, $S_{rn}$is the residual non-wetting phase saturation, and n_w and n_b are fitting parameters for wetting and non-wetting phases. Brooks-Corey models are commonly used due to its simplicity and broad application (Fig. 6.1).

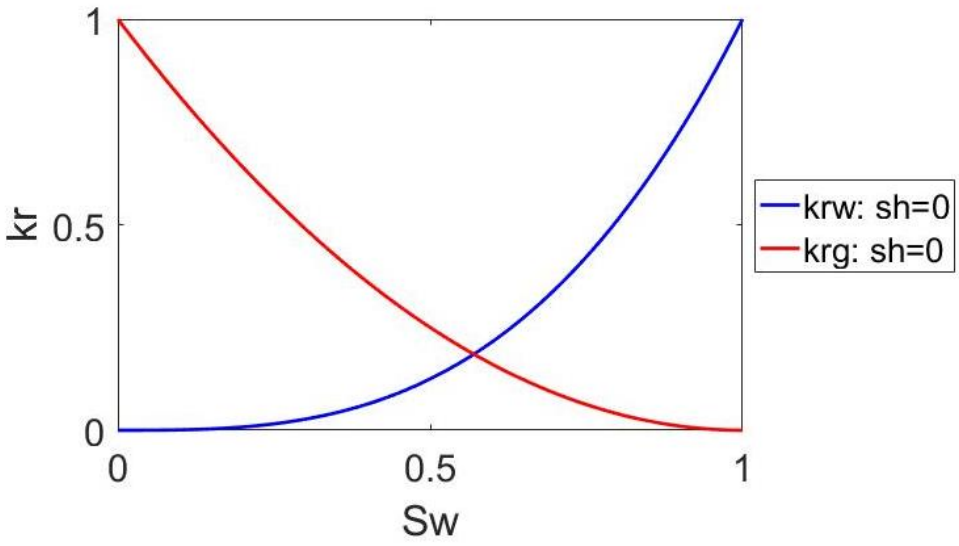

Figure 6.1. *Brooks-Corey relative permeability for gas and water with n_w = 4 and n_n = 2.*

Multiple studies have attempted to apply the principles of Brooks and Corey (1964) to hydrate systems by adding additional fitting terms and making assumptions about the pore habit of hydrate. For example, Kleinberg et al. (2003) developed a method to determine the reduction in permeability (relative permeability) of water due to hydrate saturation. A model was developed to determine the porosity and permeability reduction caused by either pore coating (3) or pore filling (4) hydrate:

$$k_{r,w} = k_{abs}\left[1 - S_h^2 + \frac{2(1 - S_h^2)^2}{\log(S_h)}\right] \quad (3)$$

$$k_{r,w} = k_{abs}(1 - S_h)^2 \quad (4)$$

These models give an expected drop in permeability caused by a certain hydrate saturation (Fig. 6.2).

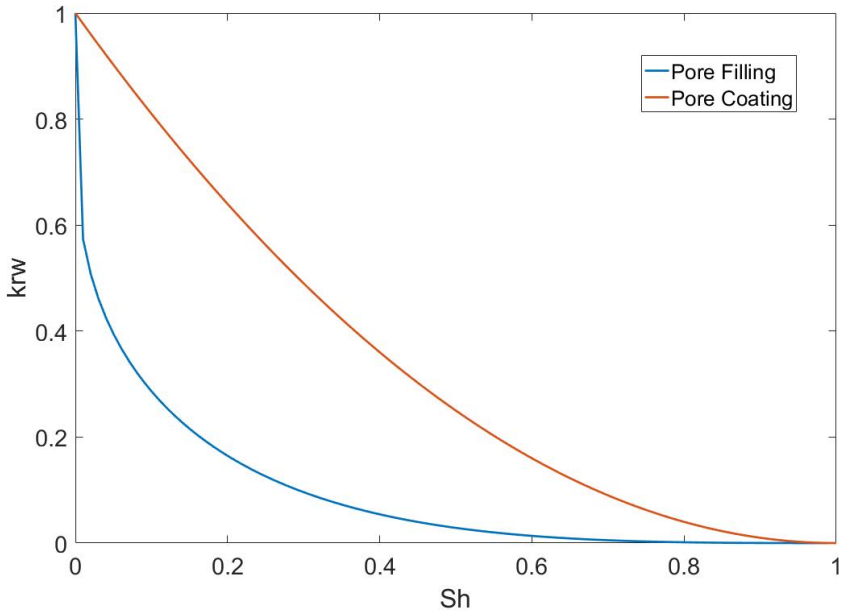

Figure 6.2. *Modeled reduction in permeability (relative permeability) due to the presence of hydrate as a pore filling or pore coating phase* (Kleinberg et al., 2003)*. Red line is from eq. 3, and blue line is from eq. 4.*

This approach has many shortcomings, including an unrealistic representation of hydrate growth in the pore network and a wide range of possible relative permeabilities at a particular hydrate saturation. Despite its shortcomings, the Kleinberg method is still the primary method used to model relative permeability in a hydrate system.

Two-phase relative permeability

A Berea Sandstone core was selected since the permeability (~220 mD) is comparable to marine sediment that is of interest to the hydrate community. Before hydrates were formed, the complete drainage gas-water relative permeability curve was measured, a key step that no other hydrate relative permeability experiments have conducted (Figure 6.3). Gas-water relative permeability for Berea Sandstone has been well studied and provides a good database to confirm and compare results. Using Darcy's Law (5) and the Darcy-Buckingham equation (6), the relative permeability was measured for a two-phase system (gas and water) (Fig. 6.3).

$$k_{abs} = \frac{Q \cdot \mu}{A}\left(\frac{L}{\Delta P}\right) \quad (5)$$

$$k_{r,i} = \frac{Q_i \cdot \mu_i}{A \cdot k_{abs}}\left(\frac{L}{\Delta P_i}\right) \quad (6)$$

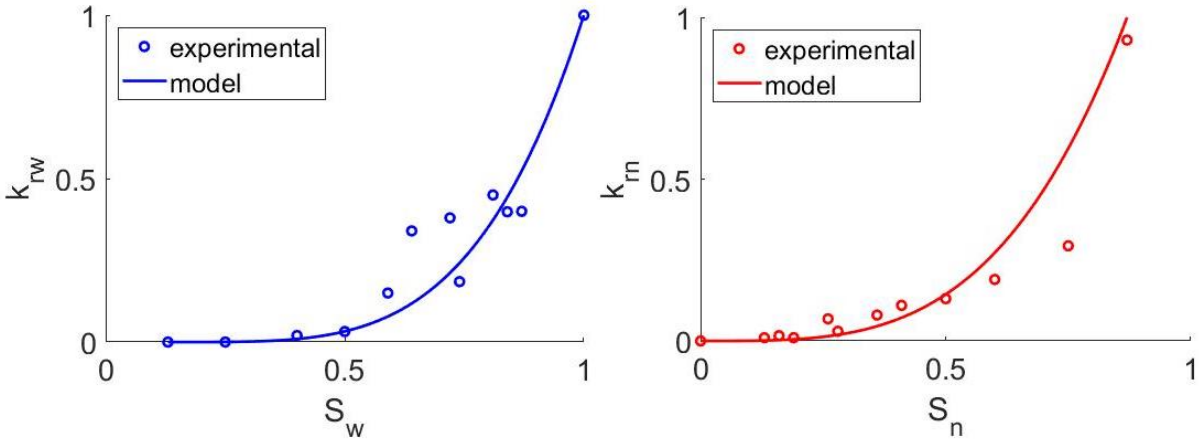

Figure 6.3. Two-phase (gas/water) relative permeability for a Berea Sandstone core.

Hydrates were formed in a pressure vessel and an estimated hydrate saturation of 25% was achieved (Murphy, 2018; Appendix A). Water was flowed through the sample until only water and hydrate remained. Once steady-state was achieved, the pressure drop was measured. The resulting relative permeabilities are shown in Fig. 6.4.

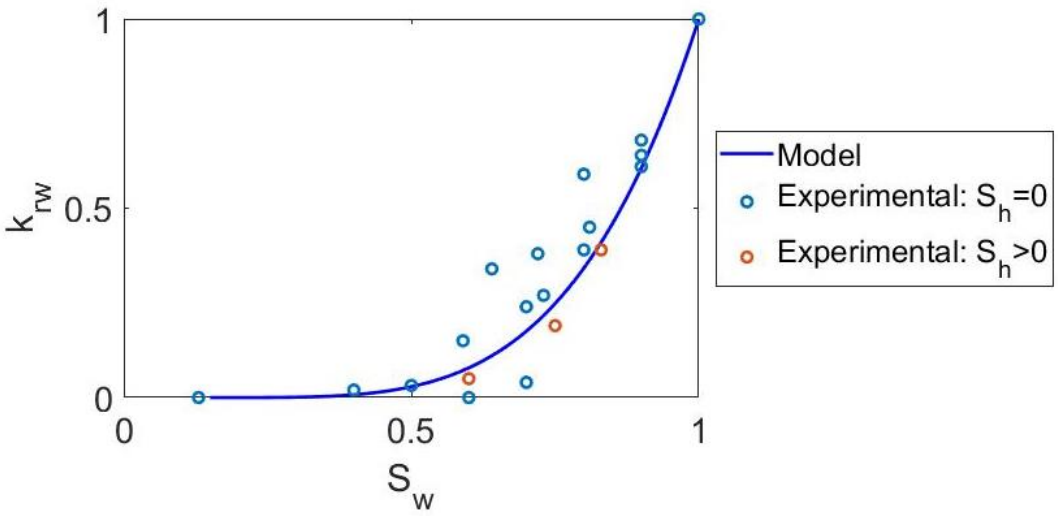

Figure 6.4. Water relative permeability for a Berea Sandstone without (blue) and with (red) hydrate. For the hydrate experiments, there was no free gas present in the sample, meaning it is at two-phase conditions.

Discussion

In a two-phase system with hydrate and water, water is the wetting phase and therefore occupies the smallest pores in a water wet media. A two-phase hydrate/water scenario should behave similarly to a gas/water or water/oil relative permeability and can therefore be modeled with Brooks-Corey. Early experiments have shown that hydrate/water behavior is consistent with gas/water. Hydrate or gas will occupy the largest pores and water will occupy the smaller pores. This behavior should not change if hydrate replaces gas as the non-wetting phase. Therefore, by measuring the two-phase gas/water relative permeability of a porous media, the water/hydrate relative permeability of the rock can be modeled. At any hydrate saturation, the water relative permeability will fall along the two-phase gas/water relative permeability (Fig. 6.5). This fundamental understanding has been missing from the current hydrate literature.

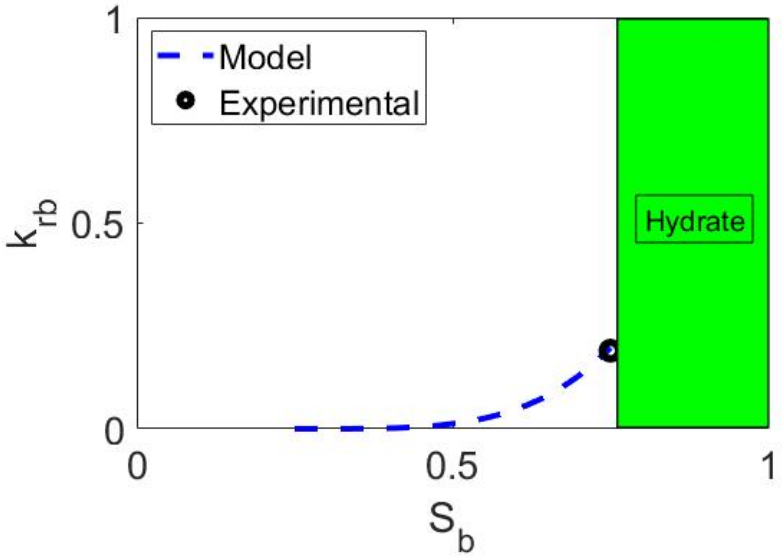

Figure 6.5. *Brine relative permeability with hydrate filling the largest 25% of pores. Blue dashed line is the model prediction. The black circle represents the measured value.*

Three-phase relative permeability

Our proposed approach for modeling three-phase (hydrate, gas, and water) relative permeability is to use the Saturation Weighted Interpolation (SWI) method. For the intermediate phase, the SWI method uses the two endmember relative permeability curves and weights them depending on the other two-phase saturations (e.g. brine and hydrate).

For example, if $S_h = 0.25$, then $k_{r,w} \approx 0.13$. The scaled Brooks-Corey model can be determined by combining equation 1 and 2 with equation 3 (pore filling) (Fig. 6.6). This scaled model is:

$$k_{r,w} = \left(\left(\frac{S_w - S_{r,w}}{1 - S_{r,w}}\right)^{n_w}\right) \cdot \left(k_{abs}\left[1 - S_h^2 + \frac{2(1 - S_h^2)^2}{\log(S_h)}\right]\right) \quad (7)$$

$$k_{r,g} = \left(\left(\frac{S_g - S_{r,g}}{1 - S_{r,w}}\right)^{n_g}\right) \cdot \left(k_{abs}\left[1 - S_h^2 + \frac{2(1 - S_h^2)^2}{\log(S_h)}\right]\right) \quad (8)$$

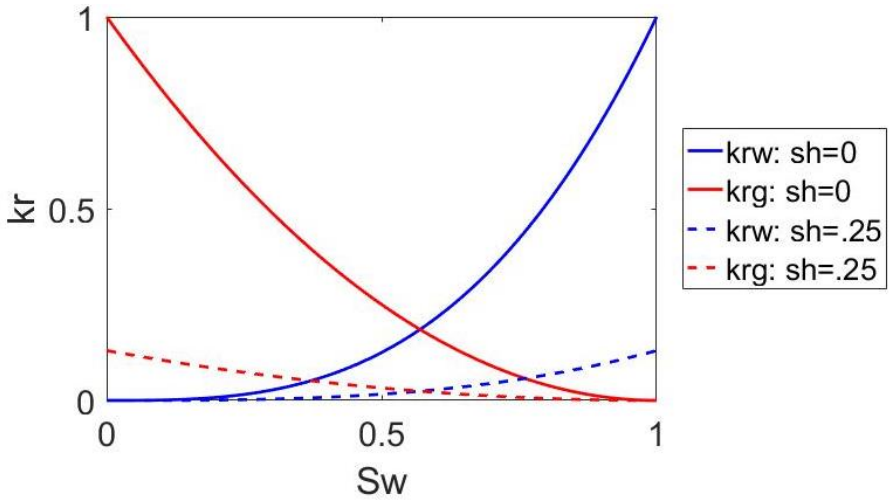

Figure 6.6. *Brooks-Corey relative permeability model without hydrate and scaled for 25% hydrate saturation* (Kleinberg et al., 2003)*. The hydrate-free Brooks-Corey model is scaled with* $k_{r,w}$*=0.13.*

Relative permeability as a function of fractional flow rate

Relative permeability is traditionally plotted as a function of water saturation. However, due to equipment limitations and difficulty in measuring three-phase saturation, the relative permeability data is plotted against the fraction flow rate of water.

$$f_w = \frac{Q_w}{Q_w + Q_g} \tag{9}$$

For experimental data, the flow rates are set throughout the experiment. Therefore, f_w is an experimental parameter that is known at all points during each experiment. However, flow rate is not a parameter in modeled relative permeability. S_w must be converted into f_w by assuming plug flow and assuming that:

$$V_{eff} = V_{pore} \cdot (1 - S_h) \tag{10}$$

$$f_w = \frac{S_w}{V_{eff}} \tag{11}$$

Since the experimental data will be plotted against f_w, all models must be converted in order to be directly compared. If the plug flow assumption is not valid, f_w can also be solved for using the Darcy-Buckingham equation (6). Combining equation (6) and (9):

$$f_w = \frac{\frac{k_{r,w}}{\mu_w}}{\frac{k_{r,w}}{\mu_w} + \frac{k_{r,g}}{\mu_g}} \tag{12}$$

The viscosity ($\mu_{w,g}$) and the relative permeability ($k_{r,(w,g)}$) are known. Therefore, the fraction flow of water (f_w) can be solved for each model. This conversion allows comparison of preliminary experimental results, but saturations must still be determined. Therefore, a system has been developed to run these experiments in the CT scanner at the UT-CT facility. These CT scans will provide phase (gas, water, hydrate) saturations.

Experimentally measured three-phase relative permeability

Experimentally measured three-phase relative permeability data was collected using the method described in Murphy, 2018. Before hydrate formation, a two-phase (gas/water) drainage relative permeability curve was measured for the sample (Fig. 6.6). Hydrates were then formed using the excess gas method. The hydrate saturation was estimated to be 25% (Appendix A). Initially, only brine was flowed through the core. The resulting values are simply endpoint relative permeability points ($f_w = 1$). Gas is then co-injected into the core to decrease the f_w value. Steady-state ($\frac{\partial P}{\partial t} = 0$)) is reached at each value of f_w. The gas and water relative permeability values are measured at each f_w until $f_w = 0$ (Fig. 6.7).

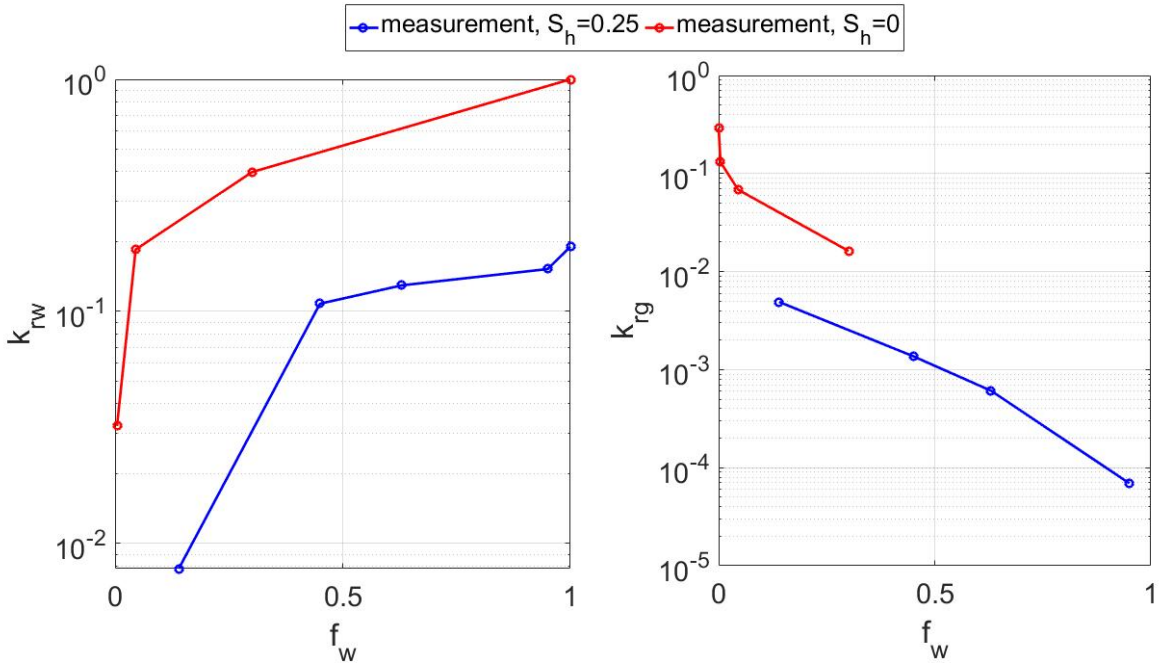

Figure 6.7. *Experimentally measured gas and water relative permeability in the presence of hydrate*$S_h = 0.25$).

Comparison with models

The experimentally derived relative permeability curves can be used to compare to the models discussed previously. Using the Kleinberg et al. (2003) scaling approach for a $S_h = 0.25$, the $k_{r,w} = 0.13$. The experimentally measured relative permeability with no hydrate is then scaled by 0.13 (Fig. 6.7).

The hydrate is the least wetting phase and will occupy the largest pore size/space. Since the relative permeability of hydrate of zero, this does not need to be modeled. For gas, the relative permeability will be a function of the water saturation and the hydrate saturation. If the water saturation is zero, the gas will be in the smallest pores and therefore the gas relative permeability will be equivalent to the two-phase water relative permeability (i.e. the gas is in the smallest pores or the wetting phase). If the hydrate saturation is zero, the gas relative permeability will be equivalent to the two-phase gas relative permeability (i.e. the gas is in the largest pores or non-wetting phase). Using these two endmembers, the gas relative permeability is interpolated between these two curves based on the water and hydrate saturation (Figure 6.8).

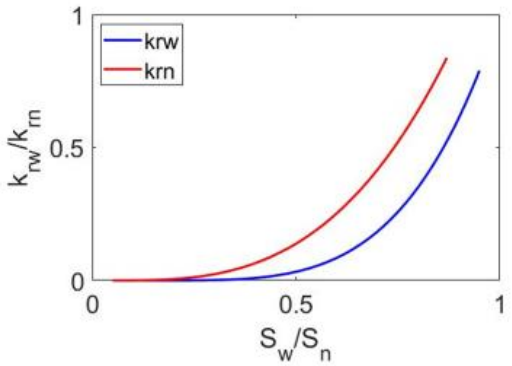

Figure 6.8. *Endmembers of gas (or oil) relative permeability in the SWI three-phase model*

Using the SWI model, the gas and water relative permeability can be modeled at any hydrate saturation. From preliminary experimental results, the SWI model seems to represent the three-phase gas and water relative permeability in the presence of hydrates (Figure 6.9).

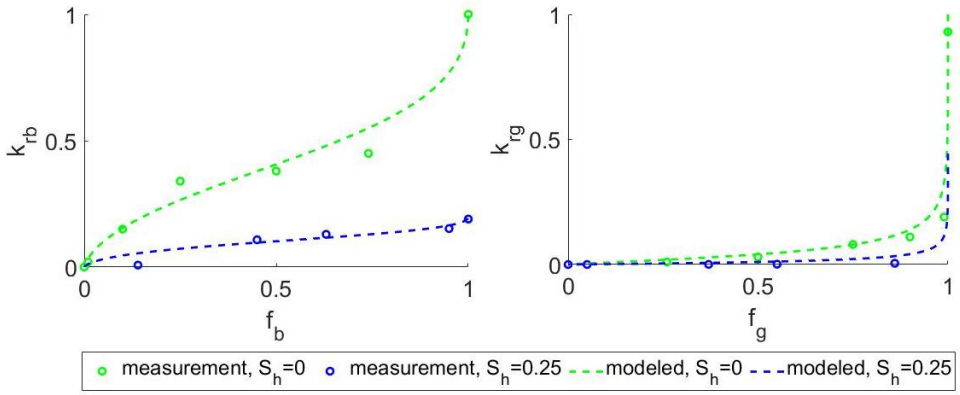

Figure 6.9. *Early experimental results for three-phase relative permeability in the presence of hydrates compared to modeled relative permeability using the SWI model.*

Task 6 references

Brooks, R.H., Corey, A.T., 1964. Hydraulic properties of porous media. Hydrology Papers 3. Colorado State University, Fort Collins.

Kleinberg, R. L., Flaum, C., Griffin, D. D., Brewer, P. G., Malby, G. E., Peltzer, E. T., & Yesinowski, J. P. (2003). Deep sea NMR: Methane hydrate growth habit in porous media and its relationship to hydraulic permeability, deposit accumulation, and submarine slope stability. *Journal of Geophysical Research -- Solid Earth*, 108(B10), 2508. https://dx.doi.org//10.1029/2003JB002389

Murphy, Z. W. (2018). Three-Phase Relative Permeability of Hydrate-Bearing Sediments. Master's Thesis. Hildebrand Department of Petroleum and Geosystems Engineering, University of Texas-Austin.

Link to actions for next Quarter, Task 6

Subtask 6.2 Steady-State Relative Permeability Measurements of Intact Pressure Cores
Planned Finish: 9/30/19
Actual Finish: Not Started

We do not anticipate that this subtask will be completed by the end of the next quarter. We are planning instead to focus our efforts on improving our technique and understanding of relative permeability in synthetic samples.

Task 7.0 Macro-Scale: Depressurization of Methane Hydrate Sand Packs and Intact Pressure Core Samples

Subtask 7.1 Depressurization of sand-pack hydrate samples
Planned Finish: 1/17/19
Actual Finish: In Progress

We completed revisions on our paper on depressurization of methane hydrate-bearing sand packs, and it was accepted in final form on June 7 (see 2. Products). We now have a better understanding of how to use these data to look at bulk density changes during depressurization.

Link to actions for next Quarter, Task 7

Subtask 7.2 Depressurization of intact pressure cores
Planned Finish: 9/30/19
Actual Finish: In Progress

We depressurized two additional core section recovered from the northern Gulf of Mexico Green Canyon 955 during UT-GOM2-1. These cores have hydrate saturations of 93% and ~76%.

We are continuing to analyze pressure rebound data from pressure core degassing experiments to look at the nature of the pressure rebound both as a pressure versus time. We observe no difference in the pressure rebound behavior between sections with an overall high saturation (coarse-grained) and low saturation (fine-grained). This lack of difference is likely due to the fact that the hydrate in fine-grained intervals is contained in thin high-saturation and coarse-grained beds and laminations. Due to the likely similarity in the pore habit between these samples, the controls on local salt and heat diffusion gradients in coarse-grained sediments at GC955 are similar in thick (tens of cm) or thin (<1 cm) beds.

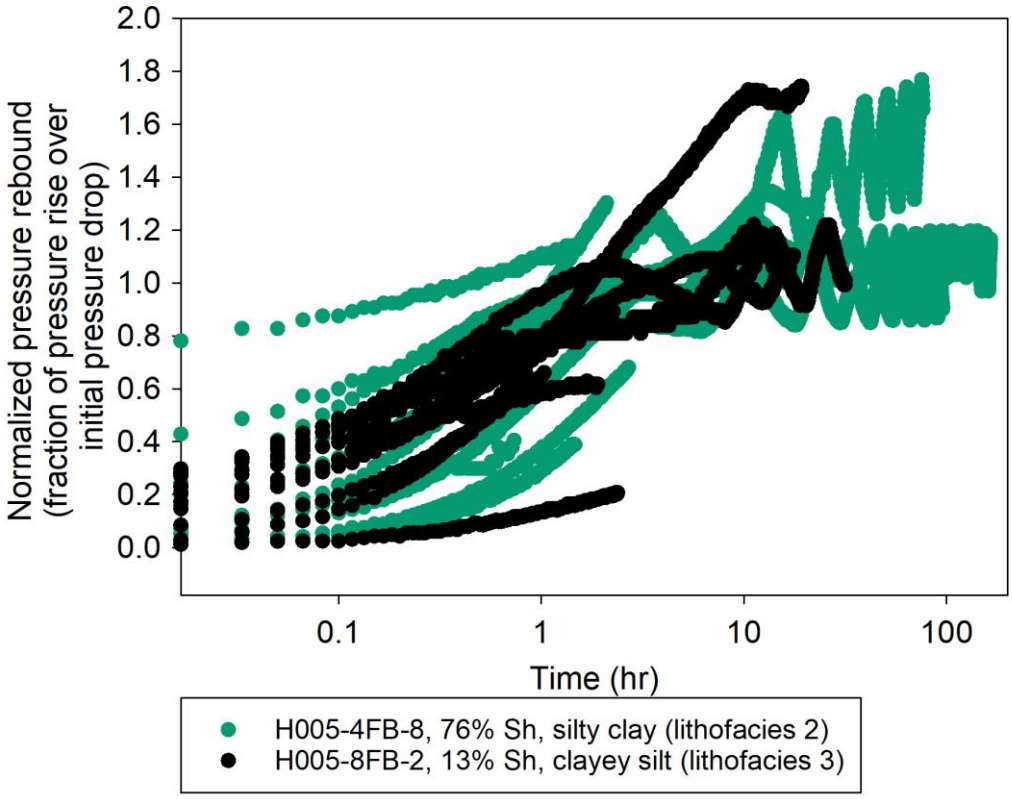

Figure 7.1 Pressure rebounds in the natural hydrate-bearing sediment sample during shut-in periods during depressurization.

Link to actions for next Quarter, Task 7

Task 8.0 Micro-Scale: CT experiments on Gulf of Mexico Sand Packs

Subtask 8.1 GOM2 Sample Preparation for Micro-CT
Planned Finish: 1/17/19
Actual Finish: In Progress

We are testing coarse sand instead of GOM2 samples due to the inability of our device to capture submicron pore geometries. A detailed rationale for this approach was provided in the quarterly report Y3Q1.

During this quarter we have prepared samples with two characteristic grain sizes (mean diameters d_{coarse} = 700 µm and d_{medium} = 150 µm). Figure 8.1 shows an example of the sand pack in the micro-consolidation cell filled with methane gas at 200 psi. The sand pack will be brought to the hydrate stability zone by (1) pressurization with KI brine under excess-water conditions to the target pressure (~8MPa), and (2) cooling after pressurization to the target temperature (~5°C). Such procedure results in a "water table" that pressurizes a "gas cap". Cycles of depressurization and pressurization help distribute methane in the sandpack to avert a clear water table. The objective of these kind of experiments is to observe directly the implications of having two different types of pore sizes on hydrate formation, pore habit, and dissociation.

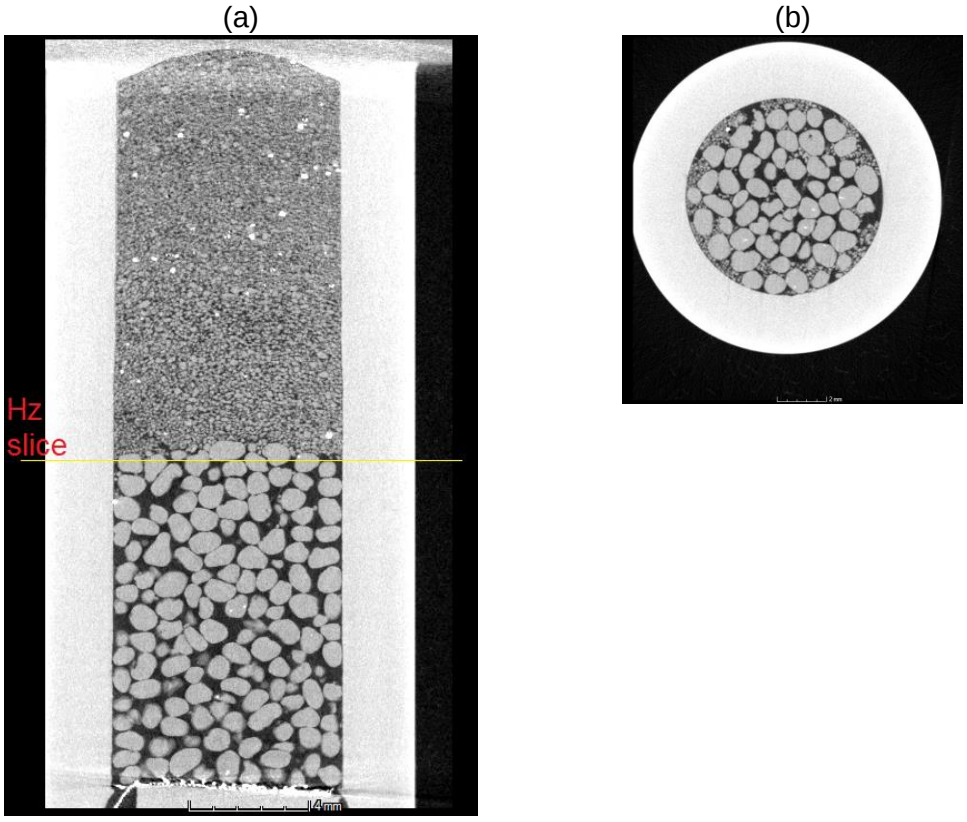

Figure 8.1. *Sand pack with two different grain sizes. (a) Vertical slice of the micro-consolidation vessel. (b) Horizontal slice near the interface of the two sand types. The objective of these experiments is to observe competing pore-size effects on hydrate formation and dissociation.*

Link to actions for next Quarter, Task 8

Subtask 8.2 Production Testing on GOM2 Samples Observed with Micro-CT
Planned Finish: 9/30/19
Actual Finish: In Progress

During this quarter we have analyzed dissociation experiments of methane hydrate in sand. The experiment follows a slow depressurization pressure-temperature path from 8.2 MPa and 6.8°C gradually to 4.3 MPa and 6.2°C over five days. Figure 8.2 shows examples of the images captured during the dissociation process. The difference between images at zero and one day(s) is negligible. Initially, CH_4 hydrate is stable and exhibits a pore-filling or pore-interconnected habit. Hydrate is porous with pores mostly filled by CH_4 gas. A few pores within hydrate and adjacent pore space is filled with high salinity brine. The increase of salinity in brine over 13 days of hydrate growth is due to ion exclusion during hydrate formation. The dissociation of the section with low hydrate saturation is straightforward (Figure 8.2 bottom). Hydrate dissociates quickly leaving water at grain contacts and releasing gas into the pore space. The case with high hydrate saturation exhibits a different and more complex behavior during dissociation. Hydrate preferentially dissociates at the boundaries of hydrate lumps. Inner hydrate may remain stable in large hydrate lumps. Over three days of dissociation, we also observe new hydrate formed where it was not present at day zero. This new hydrate is likely the result of the endothermic reaction during dissociation and the availability of relatively fresh water from dissociated hydrate (*). The fraction of interconnected pore space available to gas flow is notably small.

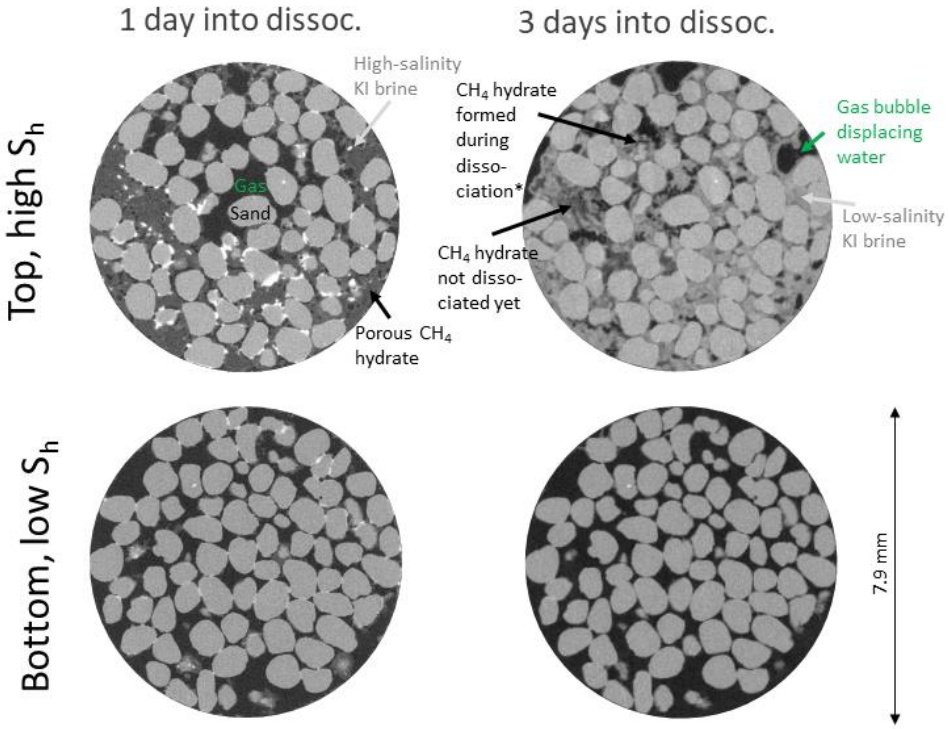

Figure 8.2. *Radial slices of micro-consolidation vessel filled with sand during hydrate dissociation under excess gas conditions. The images show that radically different scenarios occur depending on initial hydrate saturation. High initial hydrate saturation leads to complex water-gas-hydrate interactions. (*) See main text.*

Link to actions for next Quarter, Task 8

Task 9.0 Micro-Scale: Raman Observation on hydrate-bearing sand packs

Subtask 9.1 2D Imaging of methane hydrate sandpacks
Planned Finish: 3/31/2019
Actual Finish: 3/31/2019

We attempted to study the effect of capillary pressure on methane hydrate formation by synthesizing methane hydrate in a synthetic sediment pack. We first generated a dry synthetic sediment pack consisted of coarse sands (210 – 297 um in diameter) and glass beads (5 um and 80 nm in diameters) to imitate muddy sediments with capillary pressure. However, it was challenging to achieve a tight pack. The porosity was calculated to be about 80% based on grain density, which may be caused by static electricity of nano-scale glass bead powder. After injecting water into the dry glass bead pack, a significant number of voids were created within the chamber. The experiment was later aborted.

Link to actions for next Quarter, Task 9

Subtask 9.2 Micro-Raman Imaging of methane hydrate sandpacks
Planned Finish: 9/30/19
Actual Finish: In Progress

We continued to analyze the Raman data from previous methane hydrate formation experiments (RH009 and RH011). RH011 experiment was analogous to RH009 but at a slightly higher temperature. Two experiments show remarkable similarities and trends. Contrary to conventional understanding, sI methane hydrate does not form immediately. Two hours after the initial methane hydrate formation, the stoichiometry of methane hydrate is concentrated at 0.3 and 1.75. Over time, the stoichiometry is concentrated at 3, which indicates sI methane hydrate formation. Since the sI methane hydrate has a large-to-small-cage stoichiometry of 3 and the sII methane hydrate has that of 0.5, the average stoichiometry of an equal mixture of sI and sII methane hydrates is 1.75, which may explain 1.75 stoichiometry. However, the mixture of sI and sII hydrate cannot explain the low large-to-small-cage ratio of 0.3. There is no know methane hydrate structure with a large-to-small-cage ratio lower than 0.5. This may suggest a new methane hydrate structure that is thermodynamically unstable but kinetically preferred at the experimental condition. The low large-to-small-cage stoichiometry may also be explained by abundant small cages that are yet to be incorporated into well-defined methane hydrate crystals. The initially formed methane hydrate may be in a chaotic configuration of large and small cages without well-defined crystalline structures.

Link to actions for next Quarter, Task 9

C. What opportunities for training and professional development has the project provided?

We provided technical training and mentoring to one high school student and two early college-age students. These students participate in experimental design, research meetings, and experimental measurements. We continue to train two doctoral students and two post-doctoral scientists. A third post-doctoral scientist trained on this and other projects was recently promoted to research associate.

D. How have the results been disseminated to communities of interest?

- A presentation was made at the Third Deep Carbon Observatory International Science Meeting, St. Andrews, Scotland, March 23–25, 2017.
- A poster was presented at the 9th International Conference on Gas Hydrates, June 25-30, 2017, Denver, CO.
- A poster was presented at the American Geophysical Union Fall Meeting 2017, Dec. 11-15, 2017, New Orleans, LA.
- An invited talk was given at the American Geophysical Union Fall Meeting 2017, December 11-15, 2017, New Orleans, LA.
- Two posters were presented at the Gordon Research Conference- Natural Gas Hydrate Systems, 2018, Feb 25 – March 2, Galveston, TX
- Steve Phillips presented an update on HP3 at the DOE Mastering the Subsurface through Technology Innovation, Partnerships, and Collaboration: Carbon Storage and Oil and Natural Gas Technologies Review Meeting in August 2018 in Pittsburgh, PA.
- A poster was presented at the American Geophysical Union Fall Meeting 2018, Dec. 10-14, in Washington DC, titled “X-Ray Micro-CT Observation of Methane Hydrate Growth in Sandy Sediments”
- A presentation was made at the American Geophysical Union Fall Meeting 2018, Dec. 1014, 2018, in Washington DC, titled “Pore-Scale Methane Hydrate Formation under Pressure and Temperature Conditions of Natural Reservoirs”
- A poster was presented at the American Geophysical Union Fall Meeting in December 18, 2018, in Washington, D.C. titled “Three phase relative permeability of hydrate bearing sediments.”
- A poster was presented at the 8th Jackson School Research Symposium, February 2, 2019, in Austin, TX, titled “Pore-Scale Methane Hydrate Formation Under Pressure and Temperature Conditions of Natural Reservoirs”
- A poster was presented at the Austin Geological Society Research Symposium, April 1, 2018, in Austin, TX, titled “Pore-Scale Methane Hydrate Formation Under Pressure and Temperature Conditions of Natural Reservoirs”
- Nicolas Espinoza presented the work “X-Ray Micro-CT Observation of Methane Hydrate Growth and Dissociation in Sandy Sediments” at the Engineering Mechanics Institute Conference 2019 held in Pasadena, CA on June 19, 2019.

E. What do you plan to do during the next reporting period to accomplish the goals?

Task 1.0 Project Management and Planning (next quarter plans)

Planned Finish: 09/30/19
Actual Finish: In progress

- Complete the Y3Q3 Quarterly
- Update the HP3 Website
- Start Phase 2 Final report

Task 2.0 Macro-Scale: Relative Permeability of Methane Hydrate Sand Packs

Subtask 2.1 Laboratory Creation of Sand-Pack Samples at Varying Hydrate Levels
Planned Finish: 6/27/17
Actual Finish: 6/27/17

Subtask 2.2 Steady-State Permeability of Gas and Water of Sand-Pack Hydrate Samples
Planned Finish: 3/27/18
Actual Finish: 3/27/18

Task 3.0 Macro-Scale: Depressurization of Methane Hydrate Sand Packs

Subtask 3.1 Depressurization Tests
Planned Finish: 6/27/17
Actual Finish: 6/27/17

Subtask 3.2 Depressurization Tests with CAT scan
Planned Finish: 3/27/18
Actual Finish: 3/27/18

Task 4.0 Micro-Scale: CT Observation of Methane Hydrate Sand Packs

Subtask 4.1 Design and Build a Micro-CT compatible Pressure Vessel
Planned Finish: 6/27/17
Actual Finish: 6/27/17

Subtask 4.2 Micro-Scale CT Observations and Analysis
Planned Finish: 3/27/18
Actual Finish: 3/27/2018

Task 5.0 Micro-Scale: Raman Observation of Methane-Gas-Water Systems

Subtask 5.1 Design and Build a Micro-Raman compatible Pressure Vessel
Planned Finish: 6/27/17
Actual Finish: 6/27/17

Subtask 5.2 Micro-scale petrochemistry
Planned Finish: 03/21/18
Actual Finish: 3/27/18

Subtask 5.2 Diffusion kinetics of methane release
Planned Finish: 03/27/18
Actual Finish: 3/27/18

Task 6.0 Macro-Scale: Relative Permeability of Methane Hydrate Sand Packs and Intact Pressure Core Samples (next quarter plans)

Subtask 6.1 Steady-State Relative Permeability Measurements of Sand-Pack Hydrate Samples
Planned Finish: 9/30/19
Actual Finish: In Progress,

Water relative permeability at a range of hydrate saturations
The first task is to further test and confirm if the Brooks-Corey model accurately models water relative permeability in the presence of different hydrate saturations. I will now form hydrates at multiple (>5) saturations and measure the water relative permeability at each S_h. These experiments will produce a more robust, experimentally verified $k_{r,w}(S_h)$. If the Brooks-Corey model can be used to model relative permeability in a hydrate system, this

would significantly simplify hydrate simulations and improve our understanding of flow in these reservoirs. This relationship will also help determine if the hydrate formed is pore coating or pore filling.

Gas-water relative permeability in the presence of hydrates
After determining the two-phase relative permeability, measurements of three-phase relative permeability can be made. Three-phase relative permeability can be measured and compared with modeled relative permeability as shown in 1.6. A gas-water relative permeability curve can be made for a range of hydrate saturations. These experimentally derived models can be compared with Kleinberg models, scaled Brooks-Corey models, Van Genuchten models, etc., to determine the best method for modeling three-phase relative permeability in a hydrate-bearing reservoir.

Subtask 6.2 Steady-State Relative Permeability Measurements of Intact Pressure Cores
Planned Finish: 9/30/19
Actual Finish:

We do not anticipate completion of this task this quarter, and instead will focus on subtask 6.1.

Task 7.0 Macro-Scale: Depressurization of Methane Hydrate Sand Packs and Intact Pressure Core Samples (next quarter plans)

Subtask 7.1 Depressurization of sand-pack hydrate samples
Planned Finish: 1/17/19
Actual Finish: In Progress

We will finish analysis of CT data from the HDT-8 experiment and interpret based on dissociation stage and pressure rebound.

Subtask 7.2 Depressurization of intact pressure cores
Planned Finish: 9/30/19
Actual Finish: In Progress

We will synthesize all the results and compare the pressure rebound behavior relative to the phase boundary across the range of lithofacies and hydrate saturations, as well as compare the natural samples to the synthetic experiments. We will look at the influence of salinity, grain size, and hydrate saturation on rebound curves and

Task 8.0 Micro-Scale: CT experiments on Gulf of Mexico Sand Packs (next quarter plans)

During the last quarter of this project we will focus on the observation of methane hydrate, brine and gas habit in sands. We will also focus on how hydrate pore habit varies during dissociation. We will continue to work with coarse sands.

Subtask 8.1 GOM2 Sample Preparation for Micro-CT
Planned Finish: 1/17/19
Actual Finish: In Progress

We will use the following sands instead of GOM2 sediments: a coarse sand (~700 μm median grain diameter), and a medium-fine sand with grain size ~200 μm.

We are running these mixed-layered lithology experiments and will continue experiment execution and analysis during the next quarter.

These results will be compared to the core-scale measurements of GOM2 samples, in order to elucidate transport phenomena in hydrate systems with layered fine and coarse sequences.

Subtask 8.2 Production Testing on GOM2 Samples Observed with Micro-CT
Planned Finish: 9/30/19
Actual Finish: In Progress

- We will continue with the analysis of two methane hydrate dissociation experiments already performed. During the next quarter we will work specifically on image segmentation during dissociation.
- We will analyze the results of methane hydrate formation and dissociation in coarse sands with the water-excess method. The experiments have been already performed and digital image analysis is pending.

Task 9.0 Micro-Scale: Raman Observation on hydrate-bearing sand packs (next quarter plans)

During the last quarter of this project we will focus on investigating the role of porous media of different sizes that mimic the conditions of GOM2 Lithofacies 2 and 3, on the formation and dissociation of hydrates. This will be achieved through systematic studies of methane hydrate formation and dissociation in glass beads, natural quartz sand, and lithofacies 2 and 3. We will collaborate with Dr. Kehua You on numerical modelling of the physical processes (methane diffusion, capillary effect in porous media, length and time scale) to provide physical parameter constraints for understanding GOM2 reservoir.

Subtask 9.1 2D Imaging of methane hydrate sandpacks
Planned Finish: 6/30/19
Actual Finish: In Progress

- We will pursue the cylindrical sapphire tube design to explore methane hydrate formation and dissociation under pressure and flow gradients.
- We will develop a quantitative model to understand how grain sizes influence hydrate saturation.

Subtask 9.2 Micro-Raman Imaging of methane hydrate sandpacks
Planned Finish: 6/30/19
Actual Finish: In Progress

- We will assemble an experiment (RH012) similar to experiment RH010, but using glass beads with different grain sizes (200-300 μm vs. 40-50 μm). Such experimental configuration would avoid the strong Raman fluorescence signal from Lithofacies 2, as observed in experimental RH010. This will help us to better constrain the effect of grain sizes on hydrate distribution.

2. PRODUCTS:

What has the project produced?

a. Publications, conference papers, and presentations

Dong, T., Lin, J. F., Flemings, P. B., Polito, P. J. (2016), Pore-scale study on methane hydrate dissociation in brine using micro-Raman spectroscopy, presented at the 2016 Extreme Physics and Chemistry Workshop, Deep Carbon Observatory, Palo Alto, Calif., 10–11 Dec.

Lin, J. F., Dong, T., Flemings, P. B., Polito, P. J. (2017), Characterization of methane hydrate reservoirs in the Gulf of Mexico, presented at the Third Deep Carbon Observatory International Science Meeting, St. Andrews, Scotland, March 23–25.

Phillips, S.C., You, K., Flemings, P.B., Meyer, D.W., and Dong, T., 2017. Dissociation of laboratory-synthesized methane hydrate in coarse-grained sediments by slow depressurization. Poster presented at the 9th International Conference on Gas Hydrates, June 25–30, 2017, Denver, CO.

Chen, X., Espinoza, N., Verma, R., and Prodanovic, M. X-Ray Micro-CT Observations of Hydrate Pore Habit and Lattice Boltzmann Simulations on Permeability Evolution in Hydrate Bearing Sediments (HBS). Presented at the 2017 AGU Fall Meeting, December 11–15, 2017, New Orleans, LA.

Chen, X., & Espinoza, D. N. (2018). Ostwald ripening changes the pore habit and spatial variability of clathrate hydrate. Fuel, 214, 614–622. https://dx.doi.org// 10.1016/j.fuel.2017.11.065.

Chen, X., Verma, R., Nicolas Espinoza, D., & Prodanović, M. (2018). Pore-Scale Determination of Gas Relative Permeability in Hydrate-Bearing Sediments Using X-Ray Computed Micro-Tomography and Lattice Boltzmann Method. Water Resources Research, 54(1), 600–608. https://dx.doi.org// 10.1002/2017WR021851.

Chen, X and Espinoza, DN (2018), Surface area controls gas hydrate dissociation kinetics in porous media, Fuel, 234, 358363. https://dx.doi.org// 10.1016/j.fuel.2018.07.030.

Chen X, D. Nicolas Espinoza, Nicola Tisato, Peter B. Flemings (2018). X-Ray Computed Micro-Tomography Study of Methane Hydrate Bearing Sand: Enhancing Contrast for Improved Segmentation, Gordon Research Conference – Natural Gas Hydrate Systems, Galveston, TX.

Chen X, D. Nicolas Espinoza, Nicola Tisato, Rahul Verma, Masa Prodanovic, Peter B. Flemings, (2018). New Insights Into Pore Habit of Gas Hydrate in Sandy Sediments: Impact on Petrophysical and Transport Properties, Gordon Research Conference – Natural Gas Hydrate Systems, Galveston, TX.

Chen X, D. Nicolas Espinoza, Nicola Tisato, Peter B. Flemings (2018). “X-Ray Micro-CT Observation of Methane Hydrate Growth in Sandy Sediments,” American Geophysical Union Fall Meeting 2018, Dec. 10–14, in Washington D.C.

Dong, T., Lin, J.-F., Flemings, P.B., Gu, J.T., Liu, J., Polito, P.J., O'Connell, J. (2017). Pore-scale study on gas hydrate formation and dissociation under relevant reservoir conditions of the Gulf of Mexico, presented at the 2017 Extreme Physics and Chemistry workshop, Deep Carbon Observatory, November 4–5, Tempe, AZ.

Dong, T., Lin, J.-F., Gu, J.T., Polito, P.J., O'Connell, J., Flemings, P.B. (2017), Spatial and temporal dependencies of structure II to structure I methane hydrate transformation in porous media under moderate pressure and temperature conditions, Abstract OS53B-1188 Presented at 2017 Fall Meeting, December 11-15, New Orleans, LA.

Dong, T., Lin, J.-F., Gu, J.T., Polito, P.J., O'Connell, J., Flemings, P.B. (2018), Transformation of metastable structure-II to stable structure-I methane hydrate in porous media during hydrate

formation, poster presented at 2018 Jackson School of Geosciences Symposium, Feb. 3, 2018, Austin, TX.

Dong, T., Lin, J. -F., Flemings, P. B., Gu, J. T., Polito, P. J., O'Connell, J. (2018), Pore-scale methane hydrate dissociation in porous media using Raman spectroscopy and optical imaging, poster presented at Gordon Research Conferences on Natural Gas Hydrate Systems, Feb. 25–March 2, 2018, Galveston, TX.

Dong, T., Lin, J. -F., Flemings, P. B., Gu, J. T., Polito, P. J., O'Connell, J. (2018), Pore-Scale Methane Hydrate Formation under Pressure and Temperature Conditions of Natural Reservoirs, American Geophysical Union Fall Meeting 2018, Dec. 10-14, 2018, Washington D.C.

Meyer, D. W., Flemings, P. B., DiCarlo, D., You, K., Phillips, S. C., and Kneafsey, T. J. (2018), Experimental investigation of gas flow and hydrate formation within the hydrate stability zone. *Journal of Geophysical Research – Solid Earth*, https://dx.doi.org// 10.1029/2018JB015748.

Meyer, D. W., Flemings, P. B., DiCarlo, D. (2018), Effect of Gas Flow Rate on Hydrate Formation Within the Hydrate Stability Zone, *Journal of Geophysical Research – Solid Earth*, 123, 6263–6276. https://dx.doi.org// 10.1029/2018JB015878.

Meyer, D. W., Flemings, P.B., You, K., DiCarlo, D.A., in review, Gas flow by invasion percolation through the hydrate stability zone, *Geophysical Research Letters*.

Meyer, Dylan Whitney (2018-10-08). Dynamics of Gas Flow and Hydrate Formation within the Hydrate Stability Zone, Department of Geological Sciences, doctoral dissertation, The University of Texas at Austin, Austin, TX. https://dx.doi.org// 10.15781/T2M03ZG8H.

Murphy, Z., Fukuyama, D., Daigle, H., DiCarlo, D. (2018), Three-phase relative permeability of hydrate-bearing sediments, poster presented at the American Geophysical Union Fall Meeting, Dec. 10-14, 2018, Washington, D.C.

Phillips, S.C., Flemings, P., You, K., Meyer, D., and Dong, T., 2019. Investigation of in situ salinity and methane hydrate dissociation in coarse-grained sediments by slow, stepwise depressurization. *Marine and Petroleum Geology*, 109, 128–144. https://dx.doi.org//10.1016/j.marpetgeo.2019.06.015.

Espinoza D.N., Chen X., Luo J.S., Tisato N., Flemings P.B. “X-Ray Micro-CT Observation of Methane Hydrate Growth and Dissociation in Sandy Sediments,” presented at the Engineering Mechanics Institute Conference 2019 held in Pasadena, CA on June 19, 2019.

You, K., P.B. Flemings, A. Malinverno, T. S. Collett, K. Darnell, in review, Mechanisms of Methane Hydrate Formation in Geological System, *Reviews of Geophysics.*

b. Website(s) or other Internet site(s)

- Project SharePoint: https://sps.austin.utexas.edu/sites/GEOMech/HP3/_layouts/15/start.aspx#/SitePages/Home.aspx
- Project Website

  https://ig.utexas.edu/energy/hydrate-production-properties/

c. Technologies or techniques

Nothing to Report.

d. Inventions, patent applications, and/or licenses

Nothing to Report.

e. Other products

Research Performance Progress Report (Period ending 12/31/16)
Research Performance Progress Report (Period ending 3/31/17)
Research Performance Progress Report (Period ending 6/30/17)
Research Performance Progress Report (Period ending 9/30/17)
Research Performance Progress Report (Period ending 12/31/17)
Research Performance Progress Report (Period ending 3/31/18)
Phase 1 Report (Period ending 3/31/18)
Research Performance Progress Report (Period ending 6/30/18)
Research Performance Progress Report (Period ending 9/30/2018)
Research Performance Progress Report (Period ending 12/31/2018)
Research Performance Progress Report (Period ending 3/31/2019)

3. CHANGES/PROBLEMS:

This section highlights changes and problems encountered on the project.

a. Changes in approach and reasons for change

- Relative Permeability Experiments (Task 6): Because of limitations in experimental capabilities of the K0 permeability chamber and timing issues, we do not anticipate being able to perform gas-water relative permeability measurements on pressure core material this quarter (Subtask 6.2). We will focus our efforts instead on 3-phase relative permeability measurements on synthetic samples.

- Microscale Imaging (Task 8): Our available technology is insufficient to clearly distinguish hydrate and brine and observe hydrate pore habit in Lithofacies 2 of GOM2. With such small pore sizes (<1 μm), it would be extremely difficult to segment pore space and hydrate in these silts even doing scans with a high-resolution X-ray micro-tomograph. For this reason, we consulted with the DOE project manager R. Baker and proposed to concentrate our microCT efforts for the remainder of the project on coarser sediments in which we can distinguish CH4 hydrate clearly. Our plan is to continue to image pore habit of methane hydrate and to analyze its effect on relative permeability as planned in subtasks 8.1 and 8.2. However, we will use coarser sediments that allow for hydrate/brine segmentation and permit using X-ray to its fullest.

- Micro-Raman (Task 9): The originally designed semi-cylindrical Flow-Thru Chamber cannot be produced after several attempts in accordance with sapphire specialist Rayotek Scientific Inc., due to technical difficulty. In addition, we have developed a natural sediment chamber to receive samples for Mico-Raman directly from the Pressure Core Analysis and Transfer System (PCATS) that is now being tested.

b. Actual or anticipated problems or delays and actions or plans to resolve them

Nothing to Report.

c. Changes that have a significant impact on expenditures

Nothing to Report.

d. Change of primary performance site location from that originally proposed

Nothing to Report.

4. SPECIAL REPORTING REQUIREMENTS:

Special reporting requirements are listed below.

PAST - BUDGET PERIOD 1

Nothing to Report

CURRENT – BUDGET PERIOD 2

Nothing to Report.

5. BUDGETARY INFORMATION:

The Cost Summary is in Exhibit 1.

EXHIBIT 1 – COST SUMMARY

Baseline Reporting Quarter	Budget Period 1 (Year 1)							
	Q1		Q2		Q3		Q4	
	10/01/16-12/31/16		01/01/17-03/31/17		04/01/17-06/30/17		07/01/17-09/30/17	
	Q1	Cumulative Total	Q2	Cumulative Total	Q3	Cumulative Total	Q4	Cumulative Total
Baseline Cost Plan								
Federal Share	$ 283,497	$ 283,497	$ 82,038	$ 365,535	$ 79,691	$ 445,226	$ 79,691	$ 524,917
Non-Federal Share	$ 170,463	$ 170,463	$ 7,129	$ 177,593	$ 7,129	$ 184,722	$ 7,129	$ 191,851
Total Planned	$ 453,960	$ 453,960	$ 89,167	$ 543,128	$ 86,820	$ 629,948	$ 86,820	$ 716,768
Actual Incurred Cost								
Federal Share	$ 6,749	$ 6,749	$ 50,903	$ 57,652	$ 67,795	$ 125,447	$ 162,531	$ 287,977
Non-Federal Share	$ 10,800	$ 10,800	$ 10,800	$ 21,600	$ 10,800	$ 32,400	$ 158,478	$ 190,878
Total Incurred Cost	$ 17,549	$ 17,549	$ 61,703	$ 79,252	$ 78,595	$ 157,847	$ 321,009	$ 478,855
Variance								
Federal Share	$ (276,748)	$ (276,748)	$ (31,135)	$ (307,883)	$ (11,896)	$ (319,779)	$ 82,840	$ (236,940)
Non-Federal Share	$ (159,663)	$ (159,663)	$ 3,671	$ (155,993)	$ 3,671	$ (152,322)	$ 151,349	$ (973)
Total Variance	$ (436,411)	$ (436,411)	$ (27,465)	$ (463,876)	$ (8,226)	$ (472,101)	$ 234,188	$ (237,913)

Baseline Reporting Quarter	Budget Period 1 & 2 (Year 2)							
	Q1		Q2		Q3		Q4	
	10/01/17-12/31/17		01/01/18-03/31/18		04/01/18-06/30/18		07/01/18-09/30/18	
	Q1	Cumulative Total	Q2	Cumulative Total	Q3	Cumulative Total	Q4	Cumulative Total
Baseline Cost Plan								
Federal Share	$ 109,248	$ 634,165	$ 89,736	$ 723,901	$ 128,914	$ 852,815	$ 106,048	$ 958,863
Non-Federal Share	$ 7,342	$ 199,193	$ 19,369	$ 218,562	$ 7,342	$ 225,904	$ 31,393	$ 257,297
Total Planned	$ 116,590	$ 833,358	$ 109,105	$ 942,463	$ 136,256	$ 1,078,719	$ 137,441	$ 1,216,160
Actual Incurred Cost								
Federal Share	$ 107,216	$ 395,193	$ 154,758	$ 549,951	$ 163,509	$ 713,460	$ 161,083	$ 874,542
Non-Federal Share	$ 19,857	$ 210,735	$ 7,140	$ 217,875	$ 32,567	$ 250,442	$ 7,241	$ 257,683
Total Incurred Cost	$ 127,073	$ 605,928	$ 161,898	$ 767,826	$ 196,076	$ 963,902	$ 168,324	$ 1,132,225
Variance								
Federal Share	$ (2,032)	$ (238,972)	$ 65,022	$ (173,950)	$ 34,595	$ (139,355)	$ 55,035	$ (84,321)
Non-Federal Share	$ 12,515	$ 11,542	$ (12,229)	$ (687)	$ 25,225	$ 24,538	$ (24,152)	$ 386
Total Variance	$ 10,483	$ (227,430)	$ 52,793	$ (174,637)	$ 59,820	$ (114,817)	$ 30,883	$ (83,934)

Baseline Reporting Quarter	Budget Period 2 (Year 3)							
	Q1		Q2		Q3		Q4	
	10/01/18-12/31/18		01/01/19-03/31/19		04/01/19-06/30/19		07/01/19-09/30/19	
	Q1	Cumulative Total	Q2	Cumulative Total	Q3	Cumulative Total	Q4	Cumulative Total
Baseline Cost Plan								
Federal Share	$ 80,035	$ 1,038,898	$ 53,698	$ 1,092,596	$ 53,698	$ 1,146,294	$ 53,695	$ 1,199,989
Non-Federal Share	$ 7,581	$ 264,878	$ 7,579	$ 272,457	$ 7,579	$ 280,036	$ 19,965	$ 300,001
Total Planned	$ 87,616	$ 1,303,776	$ 61,277	$ 1,365,053	$ 61,277	$ 1,426,330	$ 73,660	$ 1,499,990
Actual Incurred Cost								
Federal Share	$ 52,733	$ 927,275	$ 30,119	$ 957,394	$ 110,620	$ 1,068,014		
Non-Federal Share	$ 7,554	$ 265,237	$ 21,498	$ 286,735	$ 7,634	$ 294,369		
Total Incurred Cost	$ 60,287	$ 1,192,512	$ 51,617	$ 1,244,129	$ 118,254	$ 1,362,383		
Variance								
Federal Share	$ (27,302)	$ (111,623)	$ (23,579)	$ (135,202)	$ 56,922	$ (78,280)		
Non-Federal Share	$ (27)	$ 359	$ 13,919	$ 14,278	$ 55	$ 14,333		
Total Variance	$ (27,329)	$ (111,264)	$ (9,660)	$ (120,924)	$ 56,977	$ (63,947)		

National Energy Technology Laboratory

626 Cochrans Mill Road

P.O. Box 10940

Pittsburgh, PA 15236-0940

3610 Collins Ferry Road

P.O. Box 880

Morgantown, WV 26507-0880

13131 Dairy Ashford Road, Suite 225

Sugar Land, TX 77478

1450 Queen Avenue SW
Albany, OR 97321-2198

Arctic Energy Office

420 L Street, Suite 305

Anchorage, AK 99501

Visit the NETL website at:

www.netl.doe.gov

1-800-553-7681